Journal of Sound and Vibration 330 (2011) 625–635

Contents lists available at ScienceDirect

Journal of Sound and Vibration

journal homepage: www.elsevier.com/locate/jsvi

On the impact noise of a drop falling on water

M.S. Howe *, N.A.A. Hagen

Boston University, College of Engineering, 110 Cummington Street, Boston, MA 02215, United States

ARTICLE INFO

Article history:
Received 27 February 2010
Received in revised form
25 August 2010
Accepted 26 August 2010
Handling Editor: Y. Auregan
Available online 16 September 2010

ABSTRACT

An analysis is made of the impact sound generated when a water droplet impinges on a nominally smooth air–water interface. Guo and Ffowcs Williams [*Journal of Fluid Mechanics* 227 (1991) 345–355] derived a mathematical representation of the sound produced in the initial period of impact of duration $\ll 1\,\mu s$. The theory of this paper is a simple extension of their method that covers all of the effective life time ($\sim 100\,\mu s$) of the impact sound pulse. At the acoustic wavefront the predicted pressure signature in the water consists of a large impulsive peak with the directivity of an acoustic monopole source. Behind this peak lower frequency components of the sound are strongly influenced by the effective pressure-release condition on the free surface of the water, and the radiation acquires the characteristics of a much weaker dipole field (with dipole axis normal to the water interface) accompanied by a rapid decrease in wave amplitude. The dipole pressure exhibits a single cycle oscillation before decaying to evanescence about 0.1 ms after the initial impact. Predictions of the acoustic pressure spectral level are shown to be consistent with measurements available in the literature. Applications of the theory are envisaged to situations where the entrainment of air bubbles by droplets is not important, so that the impact is the dominant source of sound—for example, in estimating the contribution to the self-noise of a supercavitating vehicle from ventilating gas containing a 'spray' of small droplets impinging on the cavity gas–water interface.

1. Introduction

Small water droplets sprayed onto a gas–water interface constitute an important source of water-borne sound. The familiar example of rain generated noise in the sea has been intensively studied since the 1940s [1–25] but a proper understanding of the mechanics of sound production is important also in other contexts—such as, for example, in quantifying the influence on the self-noise of a supercavitating vehicle of entrained droplets in ventilating gas impinging on the gas–water cavity interface [26–28]. Similarly, although rain generated underwater noise contributes to the general background sea noise, it has been shown by Nystuen and colleagues [23–25] that its accurate measurement by means of an extensive array of underwater sensors can supply useful estimates of rainfall rates on the ocean for use in climate studies.

The sound is produced principally by two mechanisms [2]. The initial impact of the drop on the water interface produces a sharp-fronted acoustic pulse of overall duration less than about 0.1 ms with amplitude varying as U^3, where U is the droplet impact velocity on the water, usually equivalent to its terminal velocity in air. Under calm conditions it appears that the time scale of the pulse does not vary significantly with drop size [5,7], because the effect of increased drop size is compensated by increased terminal velocity and drop shape modification due to drag.

* Corresponding author.
E-mail address: mshowe@bu.edu (M.S. Howe).

0022-460X/$ - see front matter © 2010 Elsevier Ltd. All rights reserved.
doi:10.1016/j.jsv.2010.08.038

The entrainment of air in the wake of an impinging drop often results in the formation of a small air bubble whose volume pulsations produce a second component of the underwater sound, usually about 20 ms after the initial impact pulse. The bubble component is not always present, but it is usually the dominant source of noise when it occurs. It turns out [8,11,12,14,17–20,22] that a droplet impinging at its terminal velocity on smooth water will entrain an air bubble only for droplet diameters D in the range 0.8–1.1 mm (with corresponding terminal velocities $U\sim 3.3-4.4$ m/s), producing an acoustic spectrum that peaks at the bubble resonance frequency, generally within the limited range 13–25 kHz [29]. Larger drops have terminal velocities that are usually too large to entrain bubbles, and for $1.1\,\text{mm}<D<2.2\,\text{mm}$ only impact noise is generated at the terminal velocity. However, impact 'splashing' of a drop with $D>2.2$ mm often produces bubbles [15], but then the bubble resonance contribution to the sound is delayed by up to 35–65 ms after the arrival of the impact pulse. When D is very large (>4 mm) it appears that the amplitudes of the impact and bubble radiations are of comparable magnitudes [23,24].

Franz [2] argued erroneously that the main source of rain noise is the initial impact, because his observations implied that bubbles were not usually entrained by raindrops; other possible mechanisms (such as secondary splashes or drop vibration) not being important. Numerical investigations of the initial stages of drop impact on water reported in [4,7,16] indicate that the characteristic impact time is not critically dependent on drop size, because larger drops are flattened before impact. This and later measurements [21,30] prompted Nystuen [4] to conclude that the impact sound consists of a single cycle pulse of characteristic time $\sim 0.05-0.06$ ms, producing a broad spectral peak near 15–20 kHz. This coincidence in peak frequency with that produced by entrained bubbles led initially to disagreement about the true cause of the observed rain noise spectrum [22], but it is now generally agreed [23–25] that rain noise is dominated by the bubble radiation.

Guo and Ffowcs Williams [13] gave the first detailed analysis of the impact acoustic pulse which is applicable to the sound produced during about the first microsecond after 'touch down' on a nominally plane water surface. During this time the 'circle of contact' [7] between the water surface and the entering drop expands supersonically relative to the water and the contact region behaves as a very efficient high frequency, monopole acoustic source, with near field pressure of order $\rho_o U c_o$ (ρ_o,c_o being, respectively, the water density and sound speed), as in Nystuen's [4] earlier 'water hammer' theory. The sound generated during this initial period is uninfluenced by boundary conditions at the water surface outside the circle of contact, and radiates directly to the far field producing a 'wavefront' pressure in the water that scales as $\rho_o U^2$, independently of radiation direction. The theory fails at later times that are dominated by acoustic waves of longer wavelengths, because it is then necessary to take explicit account of the free surface 'pressure release' condition in calculating the amplitudes of these waves.

In this paper a simple modification of the Guo–Ffowcs Williams [13] theory is described that permits the calculation of the impact noise to be extended out to times encompassing the entire life span of the wave, which is typically about 0.1 ms (during which time the radius of the circle of contact typically increases to no more than about 70 percent of the radius of a spherical drop). The immediate consequence of free surface 'pressure release' is to change the effective sound source type from the monopole of [13] that governs the impact noise at the wavefront, to a much less efficient dipole, with characteristic wave amplitude scaling as $\rho_o U^2 M$ ($M=U/c_o\ll 1$), and with dipole axis normal to the mean water surface. The free surface condition is incorporated into the theory by expressing the sound in terms of an acoustic Green's function that simultaneously vanishes on the free water surface outside the expanding circle of contact between the drop and the water, and has vanishing normal derivative on the surface within the circle of contact. The sound can then be calculated provided the normal component of velocity within this circle is known. This is accomplished by introducing a simple analytical model that accounts for the rapid decrease in normal velocity after the initial impact. The predicted wave profile behind the wavefront exhibits the single cycle oscillatory behaviour anticipated by Franz [2] and observed by Nystuen [21] and others. The corresponding frequency spectrum is found to be consistent with observations of Nystuen [21] and Pumphrey [22], although in the latter case the spectral peak is attributed to bubble oscillations, which are not discussed in this paper.

The acoustic problem is formulated in Section 2. The wavefront characteristics investigated by Guo and Ffowcs Williams [13] are reviewed in Section 3. Their theory is extended in Section 4 to cover the whole of the effective life time of the impact pulse with the aid of a Green's function whose derivation is outlined in the Appendix. Typical predictions and a comparison with experiment are discussed in Section 5.

2. Formal representation of the impact noise

A water droplet impinges at normal incidence and speed U on the smooth, planar free surface of an expanse of water that occupies in the undisturbed state the region $x_1>0$ of the rectangular system $\mathbf{x}=(x_1,x_2,x_3)$ (Fig. 1). Because a large drop often suffers air-drag induced deformation before contact with the water surface, the droplet is assumed to have the form of oblate spheroid with axis of symmetry of length $2R$ (parallel to the x_1 axis) and 'horizontal' principal diameter $2\wp$. The coordinate origin O is taken at the initial point of contact of the drop with the surface, which may be assumed to occur at time $t=0$. Observation confirms that the impact sound is generated typically within the interval $0<Ut/R<0.4$ (see, e.g. [16,20–22]). This is short enough for the initial motion induced in the water to be regarded as irrotational, described by a velocity potential $\varphi(\mathbf{x},t)$, say.

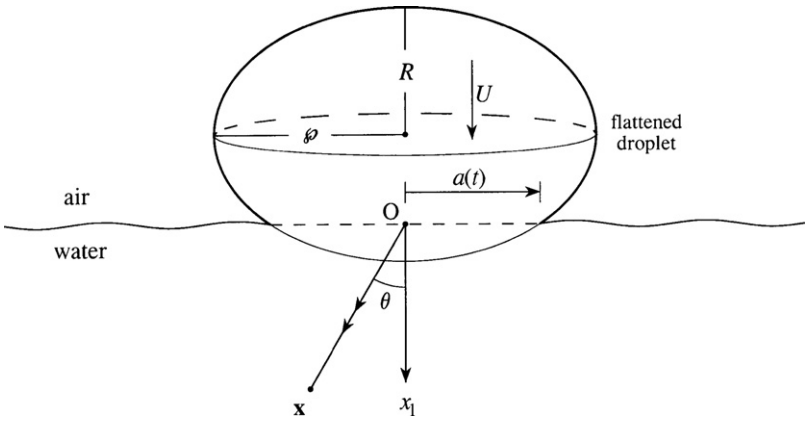

Fig. 1. Spheroidal water droplet impinging at speed U on a nominally plane air–water interface.

The characteristic Mach number $M=U/c_o \ll 1$ (where c_o is the sound speed in water), so that the impulsive motion generated in the water satisfies [31–33]

$$\left(\frac{1}{c_o^2}\frac{\partial^2}{\partial t^2}-\frac{\partial^2}{\partial x_j^2}\right)\varphi=0, \tag{1}$$

where the repeated suffix j is summed over $j=1, 2, 3$, in the usual way. The relevant solution of this equation will be sought in the region $x_1>0$ in terms of conditions on the control surface S, say, that coincides with the undisturbed free surface $x_1=0$ of the water.

To do this we introduce a Green's function $G(\mathbf{x},\mathbf{y},t,\tau)$ which satisfies (for $x_1,y_1>0$)

$$\left(\frac{1}{c_o^2}\frac{\partial^2}{\partial \tau^2}-\frac{\partial^2}{\partial y_j^2}\right)G=\delta(\mathbf{x}-\mathbf{y})\delta(t-\tau), \quad G=0 \ \text{ for } \tau>t. \tag{2}$$

In addition $G(\mathbf{x},\mathbf{y},t,\tau)$ will be required to satisfy certain conditions on the control surface S. The application of Kirchhoff's procedure [33–35] for solving the wave Eq. (1) then yields the representation

$$\varphi(\mathbf{x},t)=\int_{-\infty}^{\infty}\int_S\left(\varphi(\mathbf{y},\tau)\frac{\partial G}{\partial y_1}(\mathbf{x},\mathbf{y},t,\tau)-G(\mathbf{x},\mathbf{y},t,\tau)\frac{\partial \varphi}{\partial y_1}(\mathbf{y},\tau)\right)\mathrm{d}S\,\mathrm{d}\tau, \quad x_1>0, \tag{3}$$

where the integration is over all source times $-\infty<\tau<\infty$ and over the surface S ($y_1=0$).

3. Pressure at the wavefront

Guo and Ffowcs Williams [13] observed that during an initial interval $0<t<t_c\equiv\varepsilon^2 MR/2c_o$ of the impact the free surface of the water remains undisturbed except within the circular contact region between the drop and the water, because the radius $a(t)$ of this circle (indicated in Fig. 1) is then increasing supersonically. Reference to Fig. 1 reveals that

$$a(t)=\varepsilon\sqrt{R^2-(R-Ut)^2}, \quad \varepsilon=\frac{\wp}{R}\geq 1, \tag{4a}$$

$$\simeq\varepsilon\sqrt{2RUt} \quad \text{for } \frac{Ut}{R}<\frac{Ut_c}{R}=\frac{\varepsilon^2}{2}M^2\ll 1. \tag{4b}$$

Thus $\mathrm{d}a/\mathrm{d}t\simeq\varepsilon/2\sqrt{2RU/t}>c_o$ provided $t<t_c$. For typical rain drops t_c does not exceed a small fraction of a microsecond.

Therefore, the solution (3) can be evaluated for source times $\tau<t_c$ by taking Green's function to have the form

$$G(\mathbf{x},\mathbf{y},t,\tau)=\frac{1}{4\pi|\mathbf{x}-\mathbf{y}|}\delta\left(t-\tau-\frac{|\mathbf{x}-\mathbf{y}|}{c_o}\right)+\frac{1}{4\pi|\mathbf{x}-\overline{\mathbf{y}}|}\delta\left(t-\tau-\frac{|\mathbf{x}-\overline{\mathbf{y}}|}{c_o}\right), \tag{5}$$

where $\overline{\mathbf{y}}=(-y_1,y_2,y_3)$, which satisfies $\partial G/\partial y_1=0$ on S. The corresponding component of the acoustic pressure $p(\mathbf{x},t)\approx-\rho_o\partial\varphi(\mathbf{x},t)/\partial t$, where ρ_o is the mean density of the water, is then given by [13]

$$p(\mathbf{x},t)=\frac{\rho_o}{2\pi}\frac{\partial}{\partial t}\int_S\frac{1}{|\mathbf{x}-\mathbf{y}|}v_1\left(\mathbf{y},t-\frac{|\mathbf{x}-\mathbf{y}|}{c_o}\right)\mathrm{d}S, \tag{6}$$

where v_1 is the normal component of velocity (in the $+x_1$ direction) within the circle of contact, and the integration is confined to the region for which the retarded time satisfies

$$0 < t - \frac{|\mathbf{x}-\mathbf{y}|}{c_o} < t_c.$$

During this initial period of supersonic expansion of the circle of contact the induced motion is directed *outwards* from the interface S, in the '+' x_1 direction within the water and in the 'upwards' or '$-$' direction within the drop. Indeed, this initial motion must locally resemble that produced, respectively, by pistons with normal velocities $\pm\frac{1}{2}U$ generating locally plane pressure waves $p=\frac{1}{2}\rho_o U c_o$. It follows that the total energy radiated from the expanding circle of contact during its period of supersonic expansion is given by [13]

$$E = 2\int_0^{t_c} \pi a^2(t)\frac{1}{4}\rho_o U^2 c_o \,\mathrm{d}t = \frac{\pi}{8}\varepsilon^4 R^3 \rho_o U^2 M^3. \tag{7}$$

Half of this energy is radiated directly into the water, and half into the drop, the latter subsequently radiating into the water after multiple reflections within the drop. Guo and Ffowcs Williams [13] deduced from this that a fraction $\frac{3}{16}\varepsilon^2 M^3$ of the original kinetic energy of the impinging drop is radiated during this initial period of impact, and that this represents the dominant part of the impact radiation.

3.1. Far field acoustic pressure at the wavefront

In the acoustic far field within the water ($|\mathbf{x}|\to\infty$) on the main axis ($\theta=0$ in Fig. 1), the pressure given by (6) can be written

$$p(\mathbf{x},t) \approx \frac{\rho_o}{2\pi|\mathbf{x}|}\frac{\partial Q}{\partial t}([t]), \quad \frac{\partial Q}{\partial t}(t) = \frac{1}{2}U\pi\frac{\partial a^2}{\partial t}(t), \tag{8}$$

where $[t]=t-|\mathbf{x}|/c_o$ is the retarded time on the x_1 axis of symmetry, and Q is the effective volume source strength of the drop pushing through the interface during the supersonic phase, i.e. (using (4b)) on the main axis

$$p(\mathbf{x},t) \approx \frac{\rho_o U^2}{2}\frac{\varepsilon^2 R}{|\mathbf{x}|}, \quad |\mathbf{x}| \equiv |x_1| \to \infty, \ 0 < [t] < t_c. \tag{9}$$

This formula is valid in all radiation directions ($0<\theta<\pi/2$) at the very front $[t]\sim 0$ of the radiating pulse, which is determined by the initial volume flux from the immediate vicinity of the origin O.

4. Pressure variations to the rear of the wavefront

4.1. General formula

Components of the impact noise to the rear of the wavefront, which arrive at retarded times $[t]>t_c$, are generated when the influence of the free surface pressure release condition is important, when the dominant acoustic modes have wavelengths that become progressively larger than the retarded values of the contact radius $a([t])$. To evaluate these waves it is necessary to use the compact Green's function $G(\mathbf{x},\mathbf{y},t,\tau)$ derived in the Appendix and given explicitly in Eq. (A.9). This vanishes on the free surface $\varpi=\sqrt{y_2^2+y_3^2}>a(\tau), y_1=0$ and has vanishing normal derivative $\partial G/\partial y_1$ within the circle of contact $\varpi<a(\tau)$, $y_1=0$ of the drop and the water surface.

The acoustic pressure $p=-\rho_o\partial\varphi/\partial t$ is then determined by Eq. (3) in the form

$$p(\mathbf{x},t) \approx \frac{\rho_o\cos\theta}{\pi^2 c_o|\mathbf{x}|}\frac{\partial^2}{\partial t^2}\int_S v_1(\mathbf{y},[t])\sqrt{a^2([t])-\varpi^2}\,\mathrm{d}S, \quad |\mathbf{x}|\to\infty, \tag{10}$$

where the surface integration is over the interior of the circle of contact $\varpi<a([t])$, $y_1=0$ at the retarded time $[t]=t-|\mathbf{x}|/c_o$. There is no contribution from the first term in the integrand of (3) because $p(\mathbf{y},\tau)$, and therefore $\varphi(\mathbf{y},\tau)$, vanishes on the free surface. The result (10) describes a dipole radiation field within the water. The order of magnitude of the acoustic pressure to the rear of the wavefront $\sim\rho_o U^2 M(R/|\mathbf{x}|)$.

To evaluate the acoustic pressure from Eq. (10) requires knowledge of the evolution of the velocity v_1 at the position of the undisturbed surface of the water within the circle of contact. Following the initial period of impact of duration t_c, during which the circle of contact is expanding supersonically, acoustic disturbances within the drop bring about a rapid readjustment within the drop over a time $\sim 2R/c_o$ (typically of the order of $2-3\,\mu$s). Experiments with rain drops [20] indicate, however, that the subsequent decay from the high pressure at the wavefront of the pulse propagating in the water occurs on a larger time scale which is a small fraction of R/U, usually about 0.1 ms. This decay can be incorporated into the representation (10) by means of the following uniform approximation for the normal velocity within the circle of contact

$$v_1(\mathbf{y},\tau) = U\Psi(U\tau/R), \quad \varpi<a(\tau), \tag{11}$$

where $\Psi(U\tau/U)>0$ is a suitable function that decreases monotonically from unity at $\tau=0$. Then (10) becomes

$$p(\mathbf{x},t)\approx\frac{2\rho_o M\cos\theta}{3\pi|\mathbf{x}|}\frac{\partial^2}{\partial t^2}\left[a^3([t])\Psi\left(\frac{U[t]}{R}\right)\right],\quad |\mathbf{x}|\to\infty. \tag{12}$$

4.2. Exponential decay of normal velocity

The simplest analytical model for the normal velocity $v_1(\mathbf{y},\tau)$ within the circle of contact is obtained by setting

$$\Psi\left(\frac{Ut}{R}\right)=\mathrm{e}^{-\alpha_e Ut/R}, \tag{13}$$

where the coefficient $\alpha_e>0$ is constant. This exponential factor accounts for the rapid deceleration of the downward motion within the circle of contact. During the brief interval $0<\tau\ll R/U$ of source times in which sound is produced by the impact it will be assumed that the inertia of the water within the drop ensures that Eq. (4a) continues to be a good approximation for the radius of the circle of contact.

These hypotheses lead to a representation of the radiated pressure (12) just to the rear of the wavefront that can be cast in the form:

$$p(\mathbf{x},t)\approx\frac{\rho_o U^2}{2}\frac{\varepsilon^2 R}{|\mathbf{x}|}\frac{\frac{4}{\pi}\varepsilon M\cos\theta\mathcal{F}_e\left(\alpha_e,\frac{U[t]}{R}\right)}{\left[1-\left(\frac{U[t]}{R}-1\right)^2\right]^{1/2}},\quad |\mathbf{x}|\to\infty, \tag{14}$$

where

$$\mathcal{F}_e\left(\alpha_e,\frac{Ut}{R}\right)=\left(1+2\left[\alpha_e\left(\frac{Ut}{R}-1\right)-1\right]\left[1-\left(\frac{Ut}{R}-1\right)^2\right]+\frac{\alpha_e^2}{3}\left[1-\left(\frac{Ut}{R}-1\right)^2\right]^2\right)\mathrm{e}^{-\alpha_e Ut/R}. \tag{15}$$

The function $\mathcal{F}_e(\alpha_e,U[t]/R)$ describes the decay of the wave with increasing retarded time $[t]$ and $\mathcal{F}_e\to1$ as $[t]\to0$ at the wavefront.

4.3. Normal velocity with variable time constant

The exponential model (13) describes a constant fractional rate of decay of the normal velocity over the impact region. However, it may be more realistic to assume that the rate of decay actually increases with time elapsed from the beginning of the impact. This is certainly one interpretation of the numerical results of Nystuen [4], Nystuen and Farmer [7] and Nystuen et al. [16] for a 3 mm diameter raindrop, which exhibit a progressively rapid slowing of the absorption of the droplet into the water after about 30 μs. This situation can be simulated by the Gaussian approximation

$$\Psi\left(\frac{Ut}{R}\right)=\mathrm{e}^{-\alpha_g(Ut/R)^2}, \tag{16}$$

where $\alpha_g(Ut/R)$ plays the role of the variable time constant and α_g is a constant.

The acoustic pressure is again given by formula (14), but with $\mathcal{F}_e(\alpha_e,Ut/R)$ replaced by

$$\mathcal{F}_g\left(\alpha_g,\frac{Ut}{R}\right)=\left\{\left[\frac{Ut}{R}-1\right]^2+\left(4\alpha_g\frac{Ut}{R}\left[\frac{Ut}{R}-1\right]-1\right)\left[1-\left(\frac{Ut}{R}-1\right)^2\right]+\frac{2\alpha_g}{3}\left(2\alpha_g\left(\frac{Ut}{R}\right)^2-1\right)\left[1-\left(\frac{Ut}{R}-1\right)^2\right]^2\right\}\mathrm{e}^{-\alpha_g(Ut/R)^2}, \tag{17}$$

which satisfies $\mathcal{F}_g(\alpha_g,0)=1$.

4.4. Composite representation of the acoustic pressure

At the wavefront Eq. (14) and the same equation with $\mathcal{F}_e$ replaced by $\mathcal{F}_g$ predict the singular behaviour

$$p(\mathbf{x},t)\sim\frac{\rho_o U^2}{2}\frac{\varepsilon^2 R}{|\mathbf{x}|}\frac{\frac{4}{\pi}\varepsilon M\cos\theta}{\sqrt{2U[t]/R}},\quad \frac{U[t]}{R}\to0,\ |\mathbf{x}|\to\infty, \tag{18}$$

whereas during the initial period of impact the wavefront pressure assumes the finite level (9) predicted by Guo and Ffowcs Williams [13].

A composite formula for the acoustic pressure that provides a smooth transition between the predictions (9) and (14) is evidently supplied by

$$p(\mathbf{x},t) \approx \frac{\rho_o U^2}{2}\frac{\varepsilon^2 R}{|\mathbf{x}|}\frac{\frac{4}{\pi}\varepsilon M\cos\theta\mathcal{F}\left(\alpha,\frac{U[t]}{R}\right)}{\left(\frac{4}{\pi}\varepsilon M\cos\theta+\left[1-\left(\frac{U[t]}{R}-1\right)^2\right]^{1/2}\right)}, \quad |\mathbf{x}|\to\infty, \tag{19}$$

where $\mathcal{F}(\alpha,U[t]/R)$ denotes either of (15) and (17), respectively, for the exponential or Gaussian normal velocity decay models. This implies, for example, that on the principal axis $\theta=0$ of the dipole radiation, the transition from the wavefront to the low frequency oscillations in its wake occurs when

$$\frac{4\varepsilon M}{\pi}\sim\sqrt{\frac{2U[t]}{R}} \quad \text{i.e. when } [t]\sim\frac{16}{\pi^2}\frac{\varepsilon^2 MR}{2c_o}\approx 1.5t_c. \tag{20}$$

5. Numerical predictions for a spherical drop

Consider a nominally spherical drop of radius $R\equiv\wp=2.3$ mm impinging on water at its terminal velocity U=9.2 m/s. This case was examined experimentally by Nystuen [21] in connection with a discussion with Pumphrey [22] regarding the profile of the impact noise pulse. Fig. 2 illustrates a smoothed, hand drawn copy of the acoustic wave profile reported by Nystuen [21, Fig. 2] directly beneath the drop (along the dipole axis $\theta=0$) at $|\mathbf{x}|=1$ m below the surface.

Figs. 3 and 4 depict 'best fit' approximations to this profile predicted by the composite approximation (19) for $\theta=0$ at $|\mathbf{x}|=1$ m, respectively, for the exponential and Gaussian models when

$$\alpha_e=12 \quad \text{and} \quad \alpha_g=50. \tag{21}$$

In each case the predicted waveform is qualitatively similar to that measured by Nystuen [21]; the wavefront peak is much too large, of magnitude $\sim$96 Pa, but its duration is much less than 1 μs (cf. Eq. (20)). The subsequent single cycle oscillations are similar in the two cases, but the minimum in the Gaussian approximation (at 0.025 ms and of magnitude -2.9 Pa) is evidently closer to the experimentally observed value. Nystuen [21] also gives details of the sound pressure level frequency spectrum $20\times\log_{10}|\hat{p}(\mathbf{x},f)|$ (dB), where $\hat{p}(\mathbf{x},f)$ is the temporal Fourier transform of the far field acoustic pressure, defined by

$$\hat{p}(\mathbf{x},f)=\int_{-\infty}^{\infty}p(\mathbf{x},t)\,\mathrm{e}^{2\pi ift}\,\mathrm{d}t. \tag{22}$$

The spectrum exhibits a broad peak near f=15 kHz, and in order to make the plots in Figs. 3 and 4 the values (21) of the coefficients α_e, α_g were chosen to ensure that the corresponding theoretical spectra also peak near 15 kHz, as illustrated in Fig. 5. It is clear that of the two approximations (13) and (16) for the normal velocity decay rate, the Gaussian model (16) provides the best overall fit to the observed wave profile, and we shall henceforth consider only this case.

Nystuen's [21] measurements apparently had a resolution of at most 200 kHz, which is probably not sufficient to capture details of the wave profile of very short time scale. A tentative examination of the consequences of this frequency

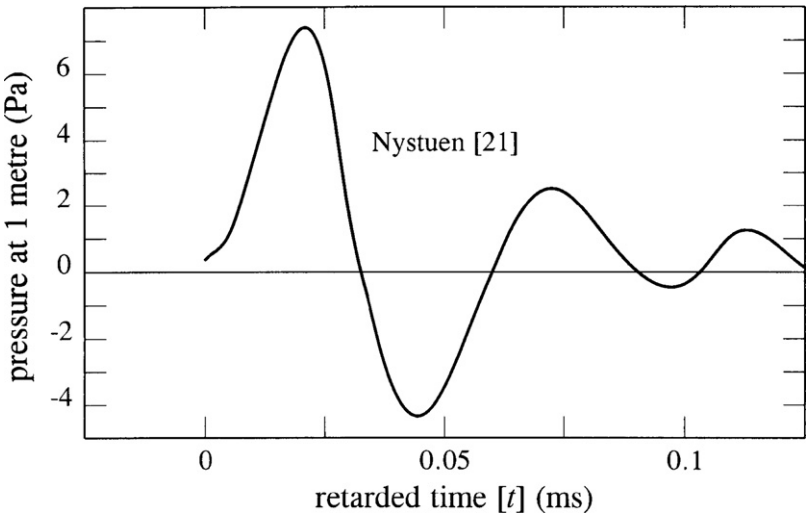

Fig. 2. Acoustic impact pressure signature (Pa) measured by Nystuen [21] at $\theta=0^{+}$, $|\mathbf{x}|=1$ m for a drop of radius R=2.3 mm impinging at U=9.2 m/s. This is a smoothed copy by hand from Fig. 2 of Nystuen's paper.

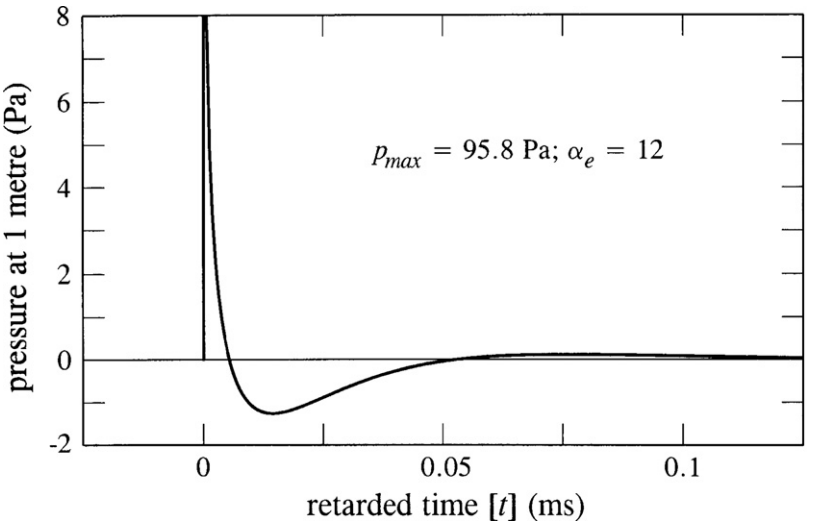

Fig. 3. Impact acoustic pressure (Pa) at $\theta = 0^\circ$, $|\mathbf{x}| = 1$ m predicted by the exponential model (13), (15), and (19) when $\alpha_e = 12$ for a drop of radius R=2.3 mm impinging on water at speed U=9.2 m/s. The large peak $p \sim 95.8$ Pa at the wavefront (Eq. (9)) is not shown.

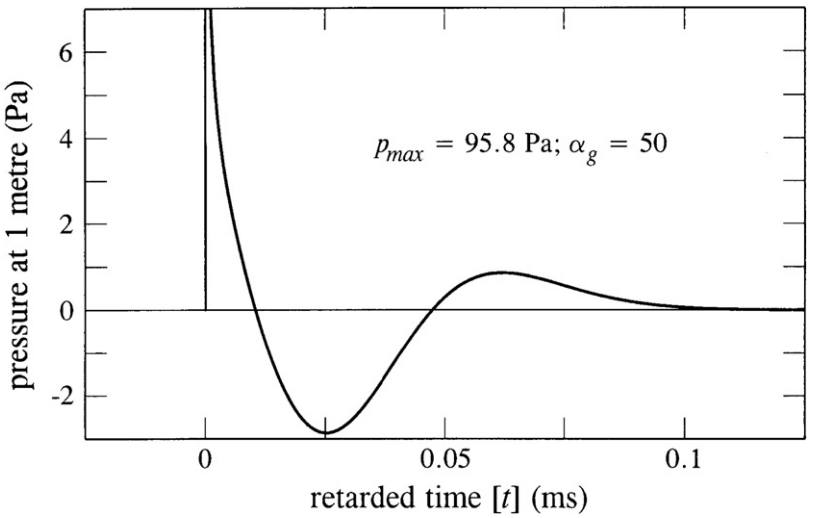

Fig. 4. Impact acoustic pressure (Pa) at $\theta = 0^\circ$, $|\mathbf{x}| = 1$ m predicted by the Gaussian model (16), (17), and (19) when $\alpha_g = 50$ for a drop of radius R=2.3 mm impinging on water at speed U=9.2 m/s. The large peak $p \sim 95.8$ Pa at the wavefront (Eq. (9)) is not shown.

limitation is obtained by calculating a 'corrected' pressure profile by Fourier inversion after first removing from the predicted Fourier transform $\hat{p}(\mathbf{x},f)$ contributions with absolute frequencies $|f| > 200$ kHz. This yields the wave profile displayed in Fig. 6 for the Gaussian model ($\alpha_g = 50$), which now exhibits a maximum pressure at the wavefront ~ 7.6 Pa, very similar to that reported by Nystuen [21] and shown in our Fig. 2.

The small scale waviness superimposed on the pressure profile of Fig. 6 is caused by the frequency cut-off at 200 kHz. The first of these 'ripples' occurs near $[t] \sim 6\,\mu$s. This type of distortion of the wavefront has previously been interpreted in terms of high frequency, multiple reflections of the initial 'water hammer' wavefront of Guo and Ffowcs Williams [13] within the drop (e.g. [15]), but it could possibly be an artifact of an inaccurate measurement procedure.

Fig. 7 illustrates the dependence of the sound pressure level frequency spectrum on the decay time-constant α_g of the Gaussian approximation (16) and (17). Three predicted spectra are plotted for $\alpha_g = 25,50,100$. Larger values of α_g produce a progressively more rapid decay of the wave pulse and shift the spectrum peak to higher frequencies. All spectra exhibit a common form at very high frequencies, where they are governed by the behaviour of the pressure very close to the wavefront, which is independent of α_g. At very high frequencies (not reached in Fig. 7, and within the region of validity of the Guo–Ffowcs Williams [13] approximation) the spectra decay like $1/f^2$. The peak for $\alpha_g = 50$ occurs at $f \simeq 15$ kHz which is close to the corresponding maximum in the spectrum measured by Nystuen [21]. It is noteworthy, however, that variations in the value of α_g, up or down by a factor of two, do not produce exceptional changes in this peak frequency.

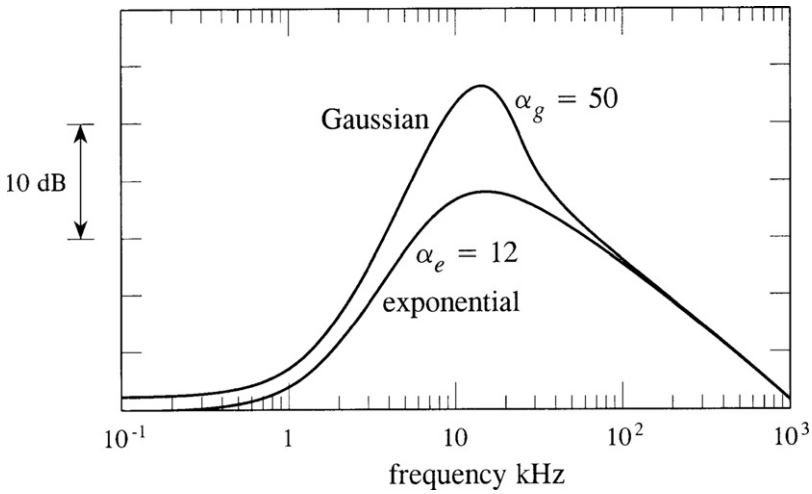

Fig. 5. Predicted acoustic pressure spectral level $20 \times \log_{10}|\hat{p}(\mathbf{x},f)|$ (arbitrary units) of the impact sound radiated at $\theta = 0^{\circ}$ by a drop of radius R=2.3 mm impinging at U=9.2 m/s: Gaussian model for $\alpha_g = 50$ and exponential model for $\alpha_e = 12$.

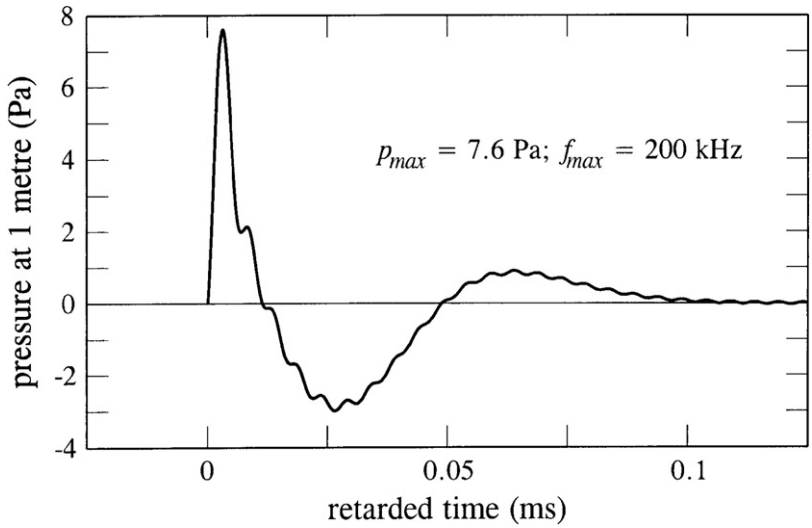

Fig. 6. Predicted acoustic pressure (Pa) at $\theta = 0^{\circ}$, $|\mathbf{x}| = 1$ m for the Gaussian model with $\alpha_g = 50$, R=2.3 mm, U=9.2 m/s when contributions to the calculated pressure at frequencies exceeding 200 kHz are omitted.

Both the *shape* of the sound pressure level spectrum and the peak frequency correspond closely to those reported by Pumphrey et al. [8] and Pumphrey [20] for the radiation from resonant volumetric oscillations of air bubbles entrained by small raindrops, typically of radii $\sim 0.4-0.55$ mm, which have resonance frequencies in the range 12–14 kHz. This correspondence is also a feature of the earlier measurements of Nystuen and Farmer [5,7]. But the two sound sources tend to be well separated in time, the resonant radiation from an entrained bubble following the impact sound after a delay of about 20 ms. The kinetic energy of such drops is very small, however, so that whenever bubble entrainment occurs the radiation is dominated by the bubble resonance. This coincidence in the frequency of small-bubble radiation and the impact noise from larger raindrops has been responsible for much confusion (see [8,11,12,14,17–19,22]).

The net acoustic energy $\mathcal{E}$ produced by the impact is determined by

$$\mathcal{E} = \int_0^{\infty} \oint_S \frac{p^2(\mathbf{x},t)}{\rho_o c_o} \, \mathrm{d}S \, \mathrm{d}t, \tag{23}$$

where the surface integral is over a large hemisphere in the water in the acoustic far field with centre at the origin and radius $|\mathbf{x}|$, and the integrals are evaluated using Eqs. (17) and (19). The upper limit of the integration with respect to the time can actually be restricted to the finite interval $0 < U[t]/R < 1$, because of the rapid exponential decay of the wave; at later times formula (4a) becomes inapplicable. For example, $U[t]/R$=1 when $[t] \simeq 2.5$ ms for the case considered above of R=2.3 mm and U=9.2 m/s.

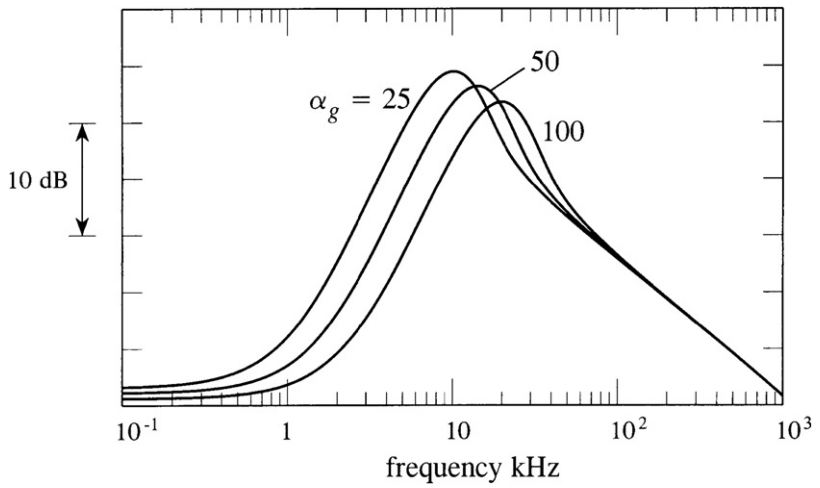

Fig. 7. Predicted acoustic pressure spectral level $20 \times \log_{10}|\hat{p}(\mathbf{x},f)|$ (arbitrary units) of the impact sound radiated at $\theta = 0^\circ$ by a drop of radius R=2.3 mm impinging at U=9.2 m/s, for the Gaussian model with $\alpha_g = 25,50,100$.

Table 1
Total radiated impact energy relative to the wavefront energy $E = \pi/8\varepsilon^4 R^3 \rho_o U^2 M^3$ [13] for a spherical drop with R=2.3 mm and U= 9.2 m/s.

α_g	25	50	100
$\mathcal{E}/E$	8.16	7.98	7.76

The calculation can be used to evaluate the ratio $\mathcal{E}/E$, where E is the total radiated energy (7) in the wavefront [13]. Results are given in Table 1 for the Nystuen experiment [21].

Similar values of $\mathcal{E}/E$ are obtained for other impact velocities U relevant to raindrops. For example, $\mathcal{E}/E \sim 10.3,8.8$, respectively, for U=3, 6 m/s.

6. Conclusion

The underwater sound produced by a drop landing on smooth water initially takes the form of a sharp pressure pulse of short duration. The wavefront of this pulse consists of a rapid pressure peak typically lasting less about a microsecond, whose strength is proportional to the drop kinetic energy. This is produced during the very initial stages of impingement of the drop on the water surface, when the radius of the circle of contact between the drop and the flat water surface is growing supersonically (relative to the sound speed in the water). The sound is then produced by a piston-like *monopole* source that is uninfluenced by the presence of the pressure-release free surface, so that the very front of the wave exhibits an amplitude that is independent of the radiation direction in the water. According to our theory the pressure decreases very rapidly behind the wavefront and acquires the characteristics of a dipole sound field (with dipole axis normal to the water interface) as soon as the pressure-release condition on the free surface begins to influence the radiation from the piston source—the rate of expansion of the contact circle is now subsonic and the characteristic wavelength of sound production rapidly becomes much larger than its radius. Within a few microseconds the dipole pressure exhibits a single cycle oscillation, becoming negative and attaining a maximum negative amplitude $\sim O(M)$ smaller than the wavefront amplitude, before finally relaxing to the steady state after attaining a small positive maximum at about 0.06 ms after the initial impact. At later times (20 ms or more after the initial impact) the sound is generally dominated by that produced by one or more bubbles entrained or produced by 'splashing impact' of the drop. It is predominantly this component of the surface interaction noise that is usually responsible for the undersea sound from rainfall, typically when raindrops have diameters exceeding about 2 mm.

The analytical theory of this paper yields predictions of the impact noise that are broadly in agreement with experiment. It should therefore be possible to estimate from the theory the contribution of 'spray' generated sound to the noise produced by the impact of ventilating gas jets on the water interface of a supercavitating underwater vehicle [26–28]. This involves high speed motion of water parallel to the interface, giving rise to the likelihood that gas jet impingement will entrain water droplets near the interface, whose subsequent convection by the jet into the water will contribute significantly to the production of jet-interface interaction noise.

Appendix A. Compact Green's function for a pressure-release free surface

Eq. (2) is to be solved for $x_1, y_1 > 0$ subject to the conditions

$$\left.\begin{array}{ll} G(\mathbf{x},\mathbf{y},t,\tau)=0 & \text{for } y_1=0, \quad \varpi > a(\tau), \\ \dfrac{\partial G}{\partial y_1}(\mathbf{x},\mathbf{y},t,\tau)=0 & \text{for } y_1=0, \quad \varpi < a(\tau), \end{array}\right\} \quad \text{where } \varpi=\sqrt{y_2^2+y_3^2}. \tag{A.1}$$

The circular domain $\varpi < a(\tau)$ is bounded by the circle of contact between the drop and the nominally plane free surface of the water at time τ (Fig. A1). The solution is required at source times for which the rate of increase of the radius $a(\tau)$ satisfies

$$\frac{1}{c_o}\frac{\partial a}{\partial \tau} \ll 1 \quad \text{i.e. for } \tau \gg t_c \equiv \frac{\varepsilon^2 MR}{2c_o}. \tag{A.2}$$

The wavelength of the generated sound is then much larger than the radius $a(\tau)$ and its production is therefore fully influenced by the pressure-release constraint on the free surface. For example: (A.2) is satisfied when $\tau > 0.1\,\mu$s for the case considered in Section 5 of a drop of radius 2.3 mm with impingement terminal velocity $U \sim 9.2$ m/s.

In the absence of the drop (when $a(\tau) \equiv 0$) we have $G = G_o$ where

$$G_o(\mathbf{x},\mathbf{y},t,\tau) = \frac{1}{4\pi|\mathbf{x}-\mathbf{y}|}\delta\left(t-\tau-\frac{|\mathbf{x}-\mathbf{y}|}{c_o}\right) - \frac{1}{4\pi|\mathbf{x}-\overline{\mathbf{y}}|}\delta\left(t-\tau-\frac{|\mathbf{x}-\overline{\mathbf{y}}|}{c_o}\right). \tag{A.3}$$

In this formula $\overline{\mathbf{y}} = (-y_1, y_2, y_3)$, and $G_o(\mathbf{x},\mathbf{y},t,\tau) = 0$ on $y_1 = 0$.

The functional form of $G(\mathbf{x},\mathbf{y},t,\tau)$ for source points $\mathbf{y}$ in the neighbourhood of the circle of contact and for an observer at $\mathbf{x}$ in the water in the acoustic far field, so that $|\mathbf{y}| \sim O(a(\tau)) \ll |\mathbf{x}|$, is found by first noting that

$$G_o(\mathbf{x},\mathbf{y},t,\tau) \simeq \frac{1}{2\pi|\mathbf{x}|}\frac{x_1 y_1}{c_o|\mathbf{x}|}\delta'\left(t-\tau-\frac{|\mathbf{x}|}{c_o}\right) \quad \text{for } |\mathbf{y}| \sim O(a(\tau)), \tag{A.4}$$

where the prime denotes differentiation with respect to the argument of the delta function.

In the presence of the expanding disc on which $\partial G/\partial y_1 = 0$ we put $G = G_o + G'$ where, for long wavelength unsteady motion close to disc, G' will be a solution of Laplace's equation $\partial^2 G'/\partial y_j^2 = 0$ that decays rapidly with distance in the water from the disc. We therefore write

$$G(\mathbf{x},\mathbf{y},t,\tau) \simeq \frac{\cos\theta}{2\pi c_o|\mathbf{x}|}(y_1 + \Phi(\mathbf{y},\tau))\delta'\left(t-\tau-\frac{|\mathbf{x}|}{c_o}\right), \tag{A.5}$$

where $\theta = \cos^{-1}(x_1/|\mathbf{x}|)$ is the radiation direction shown in Figs. 1 and A1 to the observer in the far field, and Φ is the harmonic function that vanishes at large distances from the disc and satisfies on $y_1 = 0$ the conditions

$$\Phi = 0, \quad \varpi > a(\tau), \quad \text{and} \quad 1 + \frac{\partial \Phi}{\partial y_1} = 0, \quad \varpi < a(\tau). \tag{A.6}$$

The required solution of Laplace's equation for Φ is given in Sneddon [36, pp. 76 and 77] in the form

$$\Phi = \frac{2a}{\pi}\int_0^\infty \frac{1}{k}\left[\frac{\sin(ka)}{ka} - \cos(ka)\right] J_0(k\varpi)\mathrm{e}^{-ky_1}\,\mathrm{d}k, \quad a \equiv a(\tau),\ y_1 > 0, \tag{A.7}$$

where $J_0(\cdot)$ is the Bessel function of order zero [37].

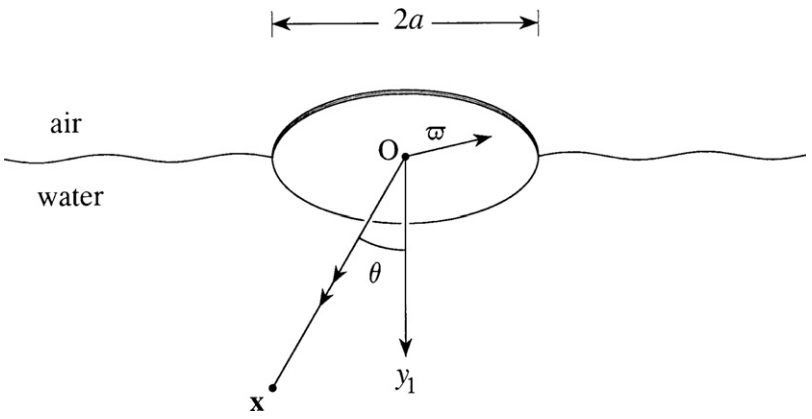

Fig. A1. Configuration defining the compact Green's function: $G = 0$ on the air–water interface; $\partial G/\partial y_1 = 0$ on the surface disc $\varpi < a(\tau)$.

By using formulae in Gradshteyn and Ryzhik [37, Section 6.693] we find

$$\Phi = \begin{cases} \dfrac{2}{\pi}\sqrt{a^2-\varpi^2} & \text{for } \varpi < a, \quad y_1 = 0, \\ 0 & \text{for } \varpi > a, \quad y_1 = 0, \end{cases} \tag{A.8}$$

and therefore that

$$G(\mathbf{x},\mathbf{y},t,\tau) \simeq \frac{\cos\theta}{\pi^2 c_o|\mathbf{x}|} H(a(\tau)-\varpi)(a^2(\tau)-\varpi^2)^{\frac{1}{2}}\delta'\left(t-\tau-\frac{|\mathbf{x}|}{c_o}\right) \quad \text{on } y_1 = 0, \tag{A.9}$$

where $H(\cdot)$ is the Heaviside unit step function.

References

[1] V.O. Knudsen, R.S. Alford, J.W. Emling, Survey of underwater sound, Report no. 3, Office of Scientific Research and Development, no. 4333, 26 September 1944.
[2] G.J. Franz, Splashes as sources of sound in liquids, *Journal of the Acoustical Society of America* 31 (1959) 1080–1096.
[3] G.W. Wenz, Acoustic ambient noise in the ocean: spectra and sources, *Journal of the Acoustical Society of America* 34 (1962) 1936–1956.
[4] J.A. Nystuen, Rainfall measurements using underwater ambient noise, *Journal of the Acoustical Society of America* 79 (1986) 972–982.
[5] J.A. Nystuen, D.M. Farmer, The influence of wind on the underwater sound generated by light rain, *Journal of the Acoustical Society of America* 82 (1987) 270–274.
[6] J.A. Scrimger, D.J. Evans, G.A. McBean, D.M. Farmer, B.R. Kerman, Underwater noise due to rain, hail and snow, *Journal of the Acoustical Society of America* 81 (1987) 79–86.
[7] J.A. Nystuen, D.M. Farmer, The sound generated by precipitation striking the ocean surface, in: B.R. Kerman (Ed.), *Sea Surface Sound*, Kluwer Academic Publishers, 1988, pp. 485–499.
[8] H.C. Pumphrey, L.A. Crum, L. Bjørnø, Underwater sound produced by individual drop impacts and rainfall, *Journal of the Acoustical Society of America* 85 (1989) 1518–1526.
[9] M.S. Longuet-Higgins, An analytic model of sound production by raindrops, *Journal of Fluid Mechanics* 214 (1990) 395–410.
[10] H.N. Oguz, A. Prosperetti, Bubble entrainment by the impact of drops on liquid surfaces, *Journal of Fluid Mechanics* 219 (1990) 143–179.
[11] H.C. Pumphrey, L.A. Crum, Free oscillations of near surface bubbles as a source of the underwater noise of rain, *Journal of the Acoustical Society of America* 87 (1990) 142–148.
[12] H.C. Pumphrey, P.A. Elmore, The entrainment of bubbles by drop impacts, *Journal of Fluid Mechanics* 220 (1990) 539–568.
[13] Y.P. Guo, J.E. Ffowcs Williams, A theoretical study on drop impact sound and rain noise, *Journal of Fluid Mechanics* 227 (1991) 345–355.
[14] H.N. Oguz, A. Prosperetti, Numerical calculation of the underwater noise of rain, *Journal of Fluid Mechanics* 228 (1991) 417–442.
[15] H. Medwin, J.A. Nystuen, P.W. Jacobus, L.H. Ostwald, D.E. Snyder, The anatomy of underwater rain noise, *Journal of the Acoustical Society of America* 92 (1992) 1613–1623.
[16] J.A. Nystuen, L.H. Ostwald Jr., H. Medwin, The hydroacoustics of a raindrop impact, *Journal of the Acoustical Society of America* 92 (1992) 1017–1021.
[17] H.N. Oguz, A. Prosperetti, Drop impact and the underwater noise of rain, in: B.R. Kerman (Ed.), *Natural Physical Sources of Underwater Sound*, Kluwer Academic Publishers, 1993, pp. 669–682.
[18] A. Prosperetti, H.N. Oguz, The impact of drops on liquid surfaces and the underwater noise of rain, *Annual Reviews of Fluid Mechanics* 25 (1993) 577–602.
[19] H.C. Pumphrey, Sources of underwater rain noise, in: B.R. Kerman (Ed.), *Natural Physical Sources of Underwater Sound*, Kluwer Academic Publishers, 1993, pp. 683–696.
[20] H.C. Pumphrey, Underwater rain noise—the initial impact component, *Acoustics Bulletin* 19 (Part 2) (1994) 19–28.
[21] J.A. Nystuen, Response to Comments on 'The hydroacoustics of a raindrop impact' [*Journal of the Acoustical Society of America* 97 (1995) 3184–3187], *Journal of the Acoustical Society of America* 97 (1995) 3188–3190.
[22] H.C. Pumphrey, Comments on 'The hydroacoustics of a raindrop impact' [*Journal of the Acoustical Society of America* 92 (1992) 1017–1021], *Journal of the Acoustical Society of America* 97 (1995) 3184–3187.
[23] J.A. Nystuen, Listening to raindrops from underwater: an acoustic disdrometer, *Journal of Atmospheric and Ocean Technology* 18 (2001) 1640–1657.
[24] B.B. Ma, J.A. Nystuen, Passive acoustic detection and measurement of rainfall at sea, *Journal of Atmospheric and Ocean Technology* 22 (2005) 1225–1248.
[25] J.A. Nystuen, E. Amitai, E.N. Anagnostou, M.N. Anagnostou, Spatial averaging of oceanic rainfall variability using underwater sound: Ionian sea rainfall experiment 2004, *Journal of the Acoustical Society of America* 123 (2008) 1952–1962.
[26] S.D. Young, T.A. Brungart, G.C. Lauchle, M.S. Howe, Effect of a downstream ventilated gas cavity on the spectrum of turbulent boundary layer wall pressure fluctuations, *Journal of the Acoustical Society of America* 118 (2005) 3506–3512.
[27] M.S. Howe, A.M. Colgan, T.A. Brungart, On self noise at the nose of a supercavitating vehicle, *Journal of Sound and Vibration* 322 (2009) 772–784.
[28] A.W. Foley, M.S. Howe, T.A. Brungart, Spectrum of the sound produced by a jet impinging on the gas–water interface of a supercavity, *Journal of Sound and Vibration* 329 (2010) 415–424.
[29] M. Minnaert, On musical air bubbles and the sounds of running water, *Philosophical Magazine Series 7* 16 (1933) 235–249.
[30] H. Medwin, A. Kurgan, J.A. Nystuen, Impact and bubble sound from raindrops at normal and oblique incidence, *Journal of the Acoustical Society of America* 88 (1990) 413–418.
[31] H. Lamb, *Hydrodynamics*, sixth ed., Cambridge University Press, 1932.
[32] J. Lighthill, *Waves in Fluids*, Cambridge University Press, 1978.
[33] M.S. Howe, *Acoustics of Fluid–Structure Interactions*, Cambridge University Press, 1998.
[34] B.B. Baker, E.T. Copson, *The Mathematical Theory of Huygens' Principle*, second ed., Oxford University Press, 1969.
[35] D.G. Crighton, A.P. Dowling, J.E. Ffowcs Williams, M. Heckl, F.G. Leppington, *Modern Methods in Analytical Acoustics*, Springer-Verlag, London, 1992.
[36] I.N. Sneddon, *Mixed Boundary Value Problems in Potential Theory*, North-Holland, Amsterdam, 1966.
[37] I.S. Gradshteyn, I.M. Ryzhik, *Tables of Integrals, Series and Products*, fifth ed., Academic Press, New York, 1994.